INTERSECTII
http://www.intersections.ro
INTERSECTIONS

Material Calibration for Static Cyclic Analyses

Andrei Crișan[1]
[1]*Department of Steel Structures and Structural Mechanics,*
Politehnica University of Timisoara, Timisoara, 300224, Romania

Summary

The material behaviour constitutive laws play a central role in the analysis of engineering components. With the focus to improve the representation of stress-strain response under non-monotonic loadings, several models for cyclic plastic deformation have been developed in recent years. Present FE commercial packages provide models for the analysis of plastic deformation of metallic materials, even though the most recent models are yet to be implemented. A combined isotropic/kinematic hardening model can be used as an extension of simple linear models. This approach provides a more accurate approximation to the stress-strain relation than the linear model. It also models other phenomena, such as ratchetting, relaxation of the mean stress and cyclic hardening, which are typical of materials subjected to cyclic loading.

Present paper presents the calibration and validation of the numerical model as part of a research project that was performed to check the validity of the moment frame connections of an 18-story steel structure. The finite element models were calibrated using experimental tests performed on four full-scale specimens at the CEMSIG Laboratory, Politehnica University Timisoara, Romania. Based on experimental test results, multiple cyclic material behavioural models were employed in order to obtain the best fitting curve.

KEYWORDS: isotropic hardening, kinematic hardening, cyclic loading, FEA

1. INTRODUCTION

Modelling the real elastic–plastic stress–strain response plays a central role in the design and failure analyses of engineering components. With the focus to improve the representation of stress-strain response under non-monotonic loadings, several models for cyclic plastic deformation have been developed in recent years. The need of different material models arises due to the fact that for modelling cyclic loading, uniaxial test information is not sufficient to describe the material behaviour. Experiments show that the cyclic plastic characteristics of a metallic material are different from the monotonic. Using monotonic data to analyse cyclic behaviour of a steel component may lead to significant errors.

ISSN 1582-3024

INTERSECTII
http://www.intersections.ro
INTERSECTIONS

Reliable results on the yield limit and hardening behaviour can be obtained with one rather simple experiment (i.e. uniaxial tensile test), while undertaking experiments to determine the cyclic plastic behaviour of metals is very complex procedure. One aspect to be monitored is the cyclic hardening/softening of the material. The hardening behaviour will change as the load cycles and the stress-strain behaviour may become very different from the monotonic.

Following extensive research, a large variety of constitutive models is available to describe the material behaviour of metals under cyclic loading. The theories are based on the observation of some of the characteristic experimental behaviour in cyclic plasticity. Magnus and Segle [1] examined the capabilities and limitations of some of the most commonly used models in cyclic plastic deformation.

Reviewing some of the existing material models for cyclic material behaviour, present paper presents the calibration and validation of the numerical model, as part of a research project that was performed to check the validity of the moment frame connections of an 18-story structure. The finite element models were calibrated using experimental tests performed on four full-scale specimens at the CEMSIG Laboratory, Politehnica University Timisoara, Romania.

2. MATERIAL MODELS

Araujo [2] presents the comprehensive description of existing material models together with the mathematical and mechanical background. A brief description is presented hereafter.

In order to describe the work-hardening material behaviour, an initial yielding condition, a flow rule, and a hardening rule is required. The purpose of initial hardening rule is to specify the state of stress for which plasticity will first occur.

Plastic materials have an elastic range within which they respond in a purely elastic manner. The boundary of this range, in either stress or strain space, is called the yield surface. The shape of the yield surface depends on the entire history of deformation from the reference state. The yield surface can change its size and shape in the stress space. When the yield surface expands it is said that material hardens and when it contracts it is said that material softens. If the material under consideration strain-hardens, the yield surface will change in accordance with the hardening rule (i.e. isotropic, kinematic, combined) for values of stress values beyond the initial yield point, where the yield point will rise to the new value of the stress state in the work-hardened material.

Since it is difficult to determine the exact locus of the yield surface, many yield criteria have been proposed. The most commonly used type of surfaces for steels is the von Mises kind, where two state variables are used: the kinematic and the

ISSN 1582-3024

INTERSECTII
http://www.intersections.ro

isotropic hardening variables. The kinematic variable accounts for the translation of the yield surface, while the isotropic variable accounts for its change in size or expansion. After the elastic limit is reached, the state of stress lies on the yield surface. If loading continues, hardening can be manifested in one of these two forms (or both): isotropic and kinematic. Isotropic hardening accounts for the expansion of the yield surface and kinematic hardening accounts for its translation in the deviatoric stress space.

2.1. Cyclic material models

Vast majority of cyclic material models rely on the two types of hardening rules described before i.e. isotropic and kinematic. Figure 1, a) presents the difference between isotropic and kinematic hardening for a uniaxial cycle loaded steel sample. For isotropic hardening, the yield surface remains the same shape, but expands with increasing stress (see Figure 1, b). The shape of the yield function is specified by the initial yield function and its size changes as the hardening parameter changes. The isotropic hardening rule cannot model the Bauschinger effect, nor similar responses, where a hardening in tension will lead to softening in a subsequent compression. This model implies that an initial yield surface symmetric about the stress axes will remain symmetric as the yield surface develops with plastic strains. In order to be able to account for such effects, a kinematic hardening rule must be implied. For this model, the yield surface remains the same shape and size but translates in stress space. The distance between the centres of the surfaces is defined as the back-stress or shift-stress.

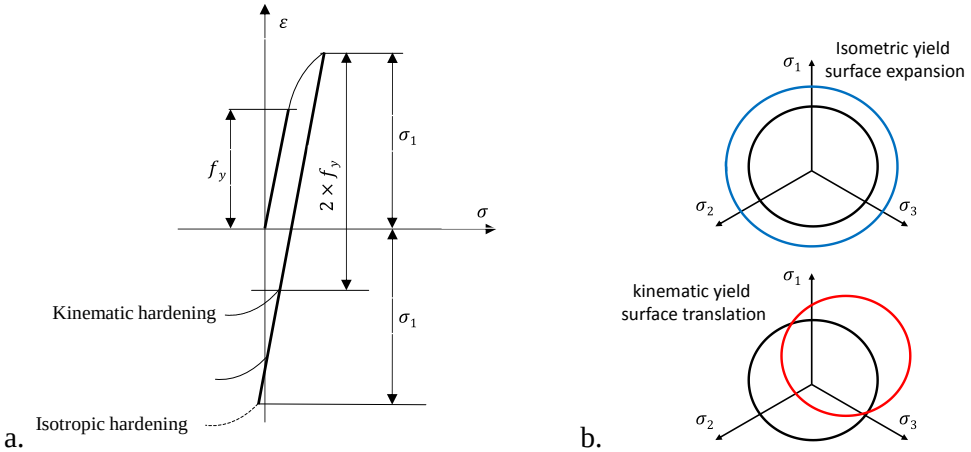

Figure 1. Isotropic/Kinematic hardening

Following, a short review of cyclic models evolution is given.

ISSN 1582-3024

Initially, Prager [3] proposed a simple kinematic hardening rule, to simulate plastic response of materials under cyclic loading. For a prescribed uniaxial stress cycle with a mean stress, the model fails to distinguish between shapes of the loading and reverse loading hysteresis curves and consequently produces a closed loop with no ratcheting. Following, Mroz [4] proposed an improvement of the linear kinematic hardening model as a multisurface model, where each surface represents a constant work hardening modulus in the stress space. Earlier, in 1958, Basseling [5], introduced a multilayer model without any notion of surfaces. Unfortunately, like the linear kinematic hardening model, multi-linear models also predict a closed loop.

Following the pioneering work of Mroz [4], new concepts of uncoupled models have been introduced by Dafalias and Popov [6]. In this model, the plastic modulus calculation is not directly dependent on the yield surface kinematic hardening rule. The kinematic hardening rule specifies the direction of movement of the yield surface centre. During a uniaxial stress cycle, the yield surface moves along the stress direction only.

Probably, the best known nonlinear kinematic hardening model has been proposed by Armstrong and Frederick [7]. The model introduces a kinematic hardening rule that contains a 'recall' term. It incorporates the fading memory effect of the strain path and essentially makes the nonlinear rule. Several improved models which are based on the Armstrong-Frederick kinematic hardening rule have been developed.

Chaboche et. al. [8], [9] proposed a 'decomposed' nonlinear kinematic hardening rule. The Chaboche rule is, in fact, a superposition of several Armstrong-Frederick hardening rules, each with its specific purpose. Ohno and Wang [10] proposed a piecewise linear kinematic hardening rule. In his thesis, Bari [11] explains that a stable hysteresis curve can be divided into three critical segments where the Armstrong-Frederick model fails and explain in detail the functionality of above mentioned models.

2.2. Kinematic models in commercial FE program, ABAQUS [12]

For numerical simulations that contains metal elements subjected to cyclic loading Abaqus [12] offers a series of kinematic hardening models. The basic concept of these models is that the yield surface shifts in stress space so that straining in one direction reduces the yield stress in the opposite direction, thus simulating the Bauschinger effect and anisotropy induced by work hardening.

The linear kinematic hardening model is the simpler of the two kinematic hardening models available in Abaqus. The evolution law of this model consists of a linear kinematic hardening component that describes the translation of the yield surface in stress space through the back-stress. It can describe stable loops in cyclic loading, including the Bauschinger effect. However, the linearity makes the

ISSN 1582-3024

INTERSECTII
http://www.intersections.ro

approximation of the Bauschinger effect rather crude. One special case of the model is the one with zero tangent modulus, which will be identical to the perfectly plastic model.

The non-linear kinematic hardening model is based on the work of Lemaitre and Chaboche [13]. The evolution law of this model consists of two components: a nonlinear kinematic hardening component, which describes the translation of the yield surface in stress space (through the back-stress) and an isotropic hardening component, which describes the change of the equivalent stress defining the size of the yield stress, as a function of the plastic deformation. In this model, the kinematic hardening component is defined to be an additive combination of a purely kinematic term and a relaxation term (the recall term), which introduces the nonlinearity.

3. CASE STUDY

3.1. Experimental tests

In order to be able to calibrate and validate the numerical model, the results of an extended experimental program were used. The experimental work presented hereafter is connected with the design of a high-rise office building, located in a high seismic area. The lateral force-resisting system was intended to create a tube-in-tube structural layout with both perimeter and core framings steel framing composed of closely spaced columns and short beams. The central core is also made of steel framing with closely spaced columns and short beams. The ratio of beam length-to-beam height, L/h, varies from 3.2 to 7.4, which results in seven different types of beams. Some beams are below the general accepted inferior limit (L/h=4). The moment frame connections employee reduced beam section (RBS) connections that are generally used for beams loaded mainly in bending.

Detailed information regarding the experimental study is presented in [15], while a brief description is presented hereafter. The columns have a cruciform cross-section made from two hot-rolled profiles of HEA800 and HEA400 section. Both beams and columns are made from S355 grade steel. The base material characteristics have been determined experimentally. The measured yield strength and tensile stress of the plates and profiles were larger than the nominal values.

Figure 2 presents the test setup. Specimens were tested under cyclic loading. The cyclic loading sequence was taken from the ECCS Recommendations [16]. Further, in Figure 5 are presented the experimental test curve used for calibration, together with the associated failure mechanism for the specimen with the RSB-S3 denomination [15].

The material properties (see Table 1) were determined using a uniaxial tensile test.

ISSN 1582-3024

Table 1. Material properties based on uniaxial tensile tests

Section	Steel grade	Element	f_y [MPa]	f_u [MPa]	A_u [%]
HEA800	S355	Flange	410.5	618.5	15.0
		Web	479.0	671.2	13.0
HEA400	S355	Flange	428.0	592.0	15.1
		Web	461.0	614.0	12.8
14 mm	S355	Beam flange	373.0	643.0	17.0
20 mm	S355	Beam web	403.0	599.0	16.5

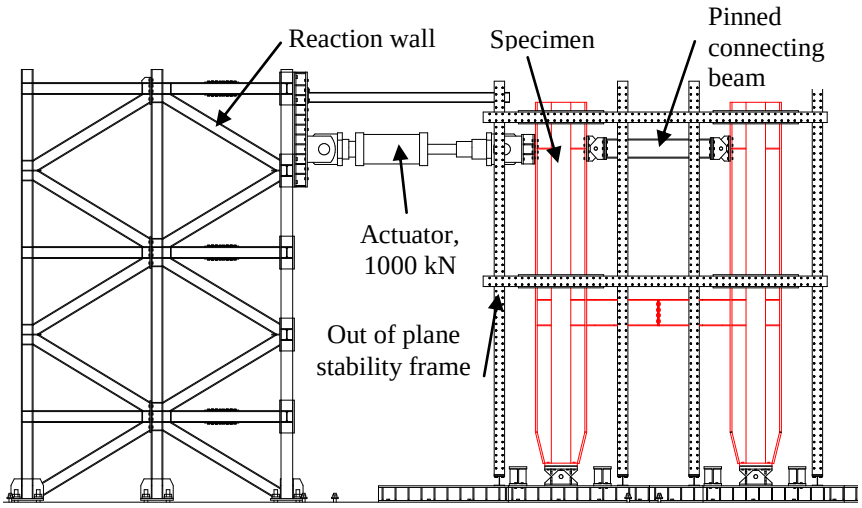

Figure 2. Test setup

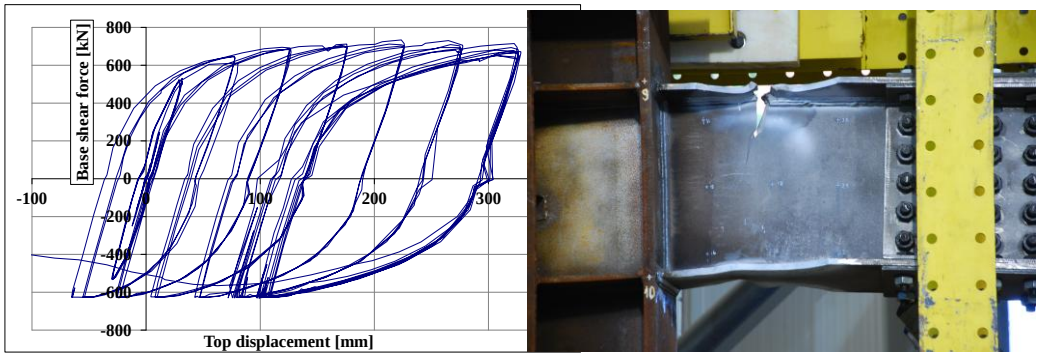

Figure 3. Experimental behaviour curve and associated failure mode

3.2. Model definition

The geometric details of the numerical model were defined using the experimental tests as reference. Considering that the stress gradient within the elements thickness (i.e. flanges, web panels, etc.) is small enough, all components were modelled as

shells and discretized using a quadratic 4-node doubly-curved "S4R" shell elements. It has to be noted that the S4R shell elements can capture the expected severe local buckling within the cross section. These elements also use reduced integration and hourglass control. The column edges at the top and bottom end are tied to the reference point using a "RIGID BODY" constraint in order to avoid local stress concentrations. At the bottom, the all three translations were blocked together with the rotation about the element axis. At the top, the rotation about element axis was blocked together with the out-of-plane translations. The axial shortening and the in-plane translations was allowed. In order to simulate pinned top connecting beam (see Figure 2), the reference points of top column constraints were tied together using a "TIE" constraint. Figure 4 presents the numerical model geometry, defined constraints, loading point and the load protocol.

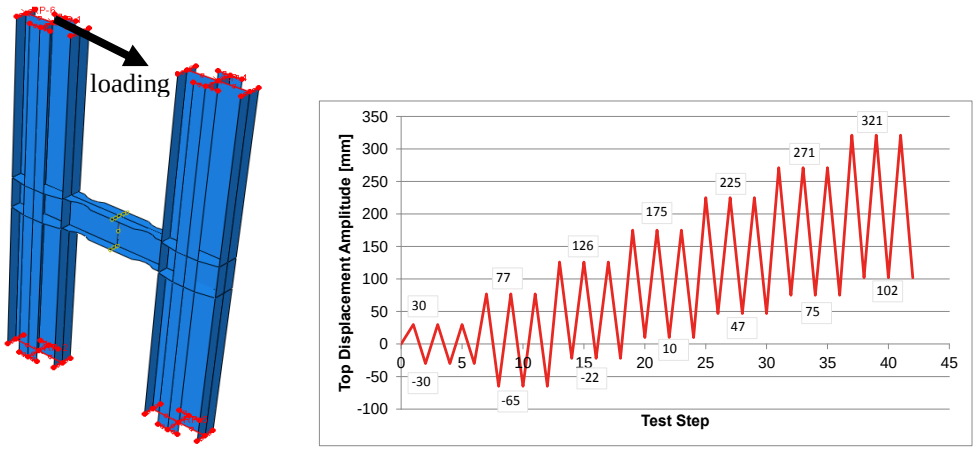

Figure 4. Geometry of numerical model and loading protocol

The load was applied at the top of left column according to the protocol presented in Figure 4.

3.3. Material calibration

Depending on the accuracy and the allowable strain required for the analysis, according to Annex C.6 of Eurocode 3 [17], the following assumptions may be used to model the material behaviour: a) elastic-plastic without strain hardening; b) elastic-plastic with a nominal plateau slope (E/10000 or similar small slope); c) elastic-plastic with linear strain hardening (E/100); d) true stress-strain curve modified from the test results as follows:

$$\sigma_{true} = \sigma(1+\varepsilon) \tag{1}$$

$$\varepsilon_{true} = \ln(1+\varepsilon) \tag{2}$$

ISSN 1582-3024

Based on the literature review presented before, multiple material modes were used to calibrate the numerical model. The elastic behaviour is modelled using the E, elastic modulus and ν, the Poisson's ratio.

3.3.1. Elastic – perfect plastic model

Usually, in structural analysis an elastic-perfect plastic model is accurate enough to model the behaviour of steel structures under monotonic loading. The parameters for an elastic-perfect plastic model are E, the elastic modulus, and the f_y yielding stress. The values used to define the elastic perfect plastic model are presented in Table 1 and in the Eurocode 3 [17]. The results of the numerical simulation, using the elastic-perfect plastic material model are presented in Figure 5.

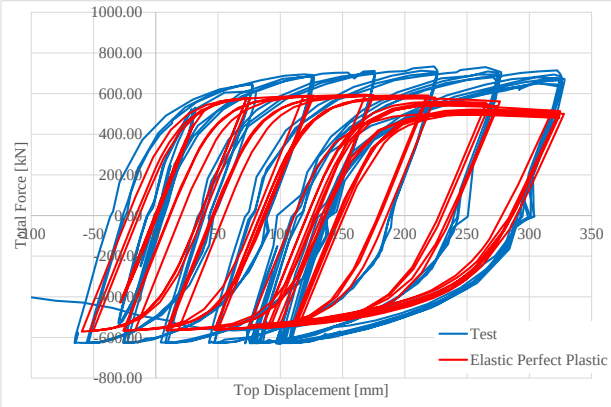

Figure 5. Experimental and numerical behaviour curves

3.3.2. Isotropic hardening model

When hardening is expected, this material model is very commonly used for metal plasticity calculations. The plasticity requires that the material satisfies a uniaxial-stress plastic-strain relationship. It use Mises yield surface with associated plastic flow, which allow for isotropic yield (increase of yield surface). This model is useful for cases involving gross plastic straining or for cases where the straining at each point is essentially in the same direction in strain space throughout the analysis.

For this model, the true stress – plastic strain was used to model the plastic material behaviour. In Figure 6 are presented the result using the isotropic hardening material model.

ISSN 1582-3024

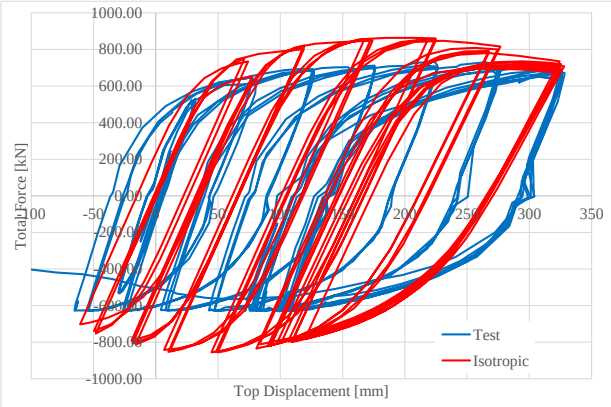

Figure 6. Experimental and numerical behaviour curves

3.3.3. Kinematic hardening model

As observed in Figure 6, the accumulation of plastic strain coupled with the inability to model the Bauschinger effect, lead to an overestimated of structural capacity. In order to solve this, a kinematic hardening model must be implied.

The true stress – plastic strain was used to model the plastic material behaviour. In Figure 7 are presented the results of the numerical simulation obtained using the kinematic hardening material model.

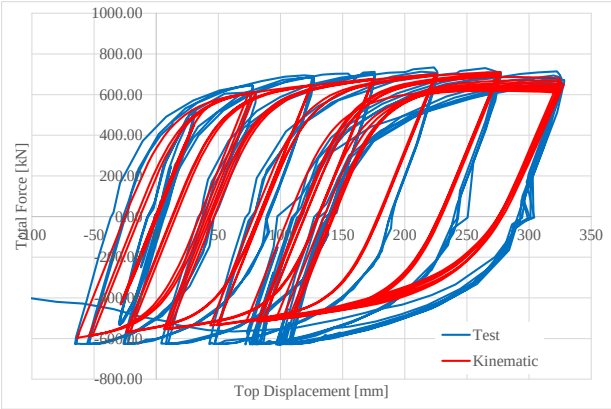

Figure 7. Experimental and numerical behaviour curves

3.3.4. Combined hardening models

Even if, the maximum load is achieved, the inability to correctly model the material hardening, resulted into underestimation of the minimum load. This nonlinear isotropic/kinematic hardening material model uses an evolution law that consists of two components: (i) a nonlinear kinematic hardening component, which

ISSN 1582-3024

INTERSECTII
INTERSECTIONS
http://www.intersections.ro

describes the translation of the yield surface in stress space through the back-stress, and (ii) an isotropic hardening component, which describes the change of the equivalent stress defining the size of the yield surface as a function of plastic deformation.

Parametric

This material model simulates the cyclic strain hardening. In addition to the modulus of elasticity (E) and the yield stress (f_y), the nonlinear kinematic and isotropic hardening components are defined. C_γ is the initial kinematic hardening modulus, γ is the rate at which C_γ decreases with cumulative plastic deformation ε_{pl}. These two parameters can be determined using the uniaxial tensile test and the values for C_γ (linear kinematic hardening modulus) and γ were determined using the formulas presented below:

$$C_\gamma = \frac{\sigma - f_y}{\varepsilon_{pl}} \tag{3}$$

$$f_u = f_y + \frac{C}{\gamma} \tag{4}$$

In Figure 8 is presented the numerical results obtained using the combined parametric hardening material model.

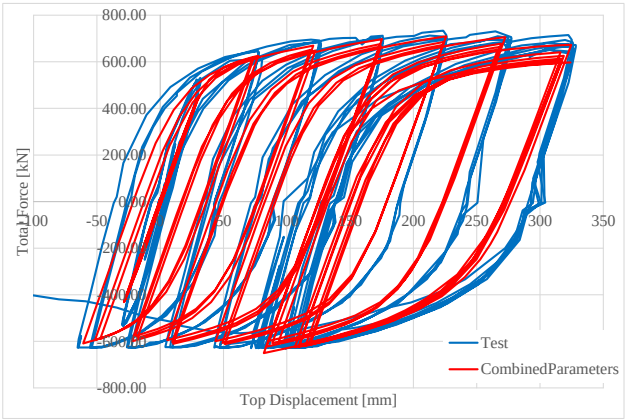

Figure 8. Experimental and numerical behaviour curves

Parametric with cyclic hardening

This material model simulates the cyclic strain hardening. In addition to the modulus of elasticity (E) and the yield stress (f_y), the nonlinear kinematic and isotropic hardening components are defined. C_γ is the initial kinematic hardening modulus, γ is the rate at which C_γ decreases with cumulative plastic deformation

ISSN 1582-3024

ε_{pl}. In addition to simple parametric model describer before, an isotropic hardening component can be defined. In Abaqus, this is defined by selecting Cyclic Hardening from the Suboptions menu. For this, the following two parameters are required: Q_{∞} – the maximum change in the size of the yield surface and b – the rate at which the size of the yield surface changes as plastic deformation develops.

Since no cyclic data for the material was available, the cyclic plastic behaviour parameters were taken from the literature. In Table 2 are presented the values considered for each model. It has to be mentioned that all considered aterial parameters were determined for carbon-steels materials.

Table2. Material properties for combined hardening material model

No.	C [MPa]	γ	Q_{∞} [MPa]	b	Reference	Results
1	25500	81	2000	0.26	[12]	Figure 11
2	2500	20	180	20	Unknown	Figure 12
3	6895	25	172	2	[18]	Figure 13
4	500000	50	20000	10	[19]	Figure 14
5	108939	2.5	-250	30	[20]	Figure 15
6	264156 20973	873 1.0	-320	30	[20]	Figure 16
7	16000	43	44	11	[21]	Figure 17

In Figure 9 to Figure 15 present the results obtained using the combined parametric hardening with cyclic hardening material model.

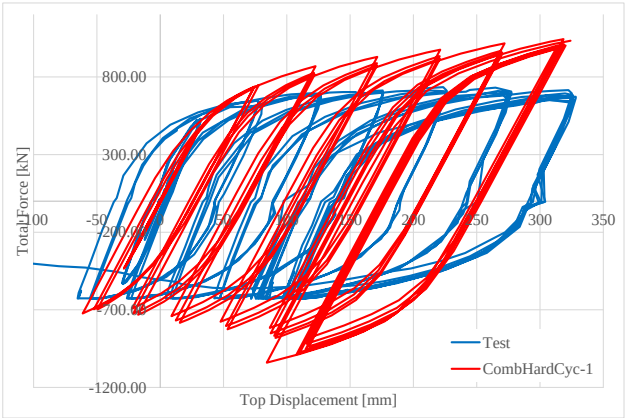

Figure 9. Experimental and numerical behaviour curves

ISSN 1582-3024

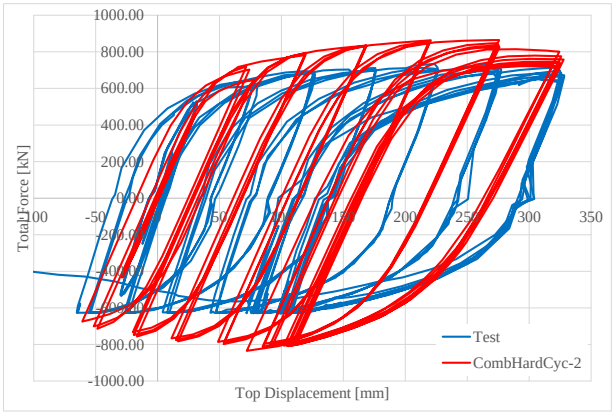

Figure 10. Experimental and numerical behaviour curves

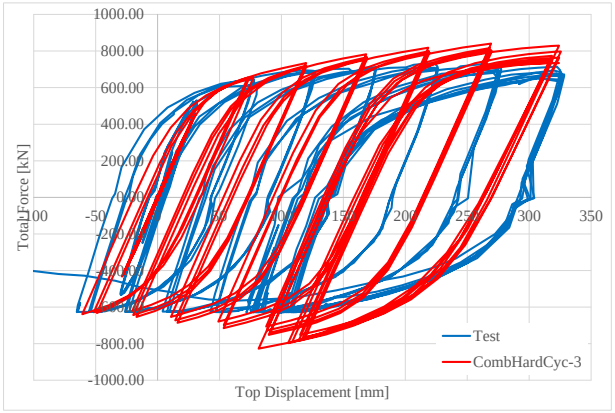

Figure 11. Experimental and numerical behaviour curves

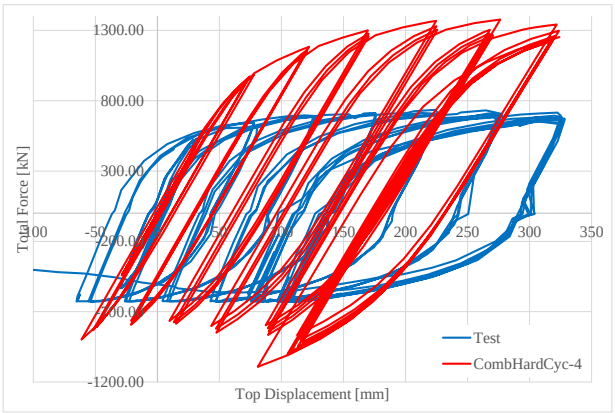

Figure 12. Experimental and numerical behaviour curves

ISSN 1582-3024

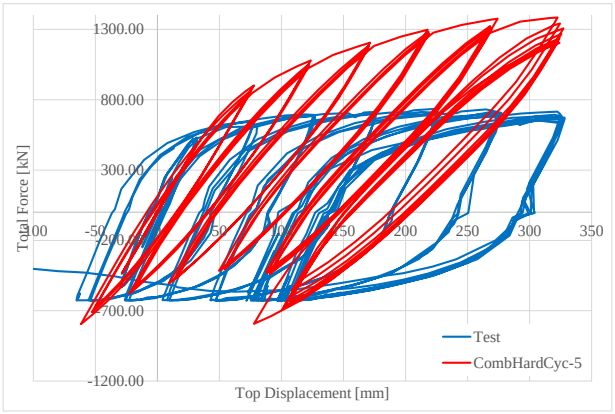

Figure 13. Experimental and numerical behaviour curves

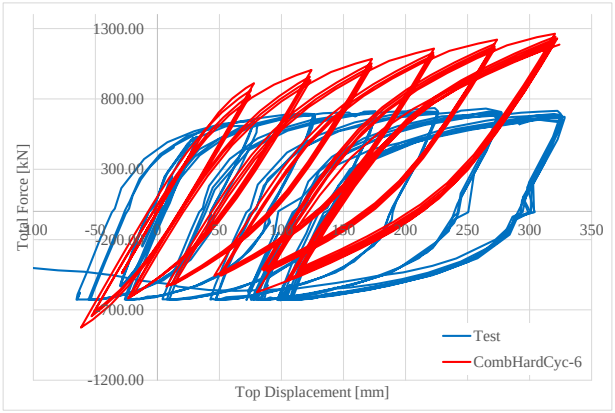

Figure 14. Experimental and numerical behaviour curves

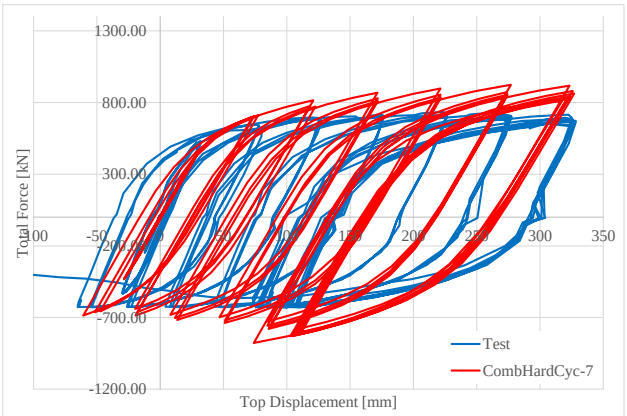

Figure 15. Experimental and numerical behaviour curves

INTERSECTII
http://www.intersections.ro
INTERSECTIONS

Half-Cycle

When limited test data are available, C_γ and γ can be based on the stress-strain data obtained from the first half cycle of a unidirectional tension or compression experiment. Using this option, Abaqus determines the values of material parameters C_γ and γ. The data used for this material model was taken from the stress – strain curve obtained for the uniaxial tensile test. This option is suitable to be used if a limited number of cycles is performed. It has to be mentioned that only the plastic component was considered and that the yielding plateau was ignored due to the fact that, during plastic cyclic loading, the yielding plateau disappear.

In Figure 18 are presented the result using the combined parametric hardening defined using the half cyclic material model.

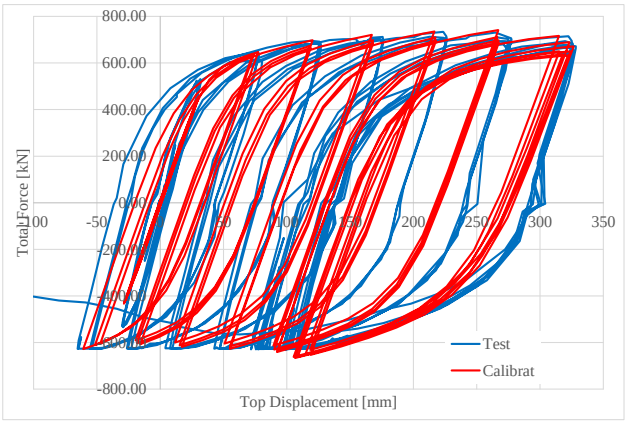

Figure 16. Experimental and numerical behaviour curves

3.3.5. Discussions

Considering the behaviour curves presented in Figure 7 – 16 it can be observed that a correct definition of material behaviour is of paramount importance when considering cyclic loading in steel structures. A simple elastic – perfect plastic material behaviour can produce very conservative results, severely underestimating the structural capacity (see Figure 5). On the other hand, considering the material isotropic hardening (Figure 6) the structural capacity is overestimated, while in case of kinematic hardening (Figure 7), the dissipated energy is underestimated.

Considering a material model that includes a combined isometric/kinematic hardening gives a very good approximation of structural behaviour. For this, two approaches can be considered, as presented in Figure 8 and Figure 16. It has to be underlined the importance of correct determination for all parameters included in material definition.

As presented in Figure 9 to Figure 15, the use of material parameters calibrated by other researchers can give unsatisfactory results for a given structure.

ISSN 1582-3024

INTERSECTII
INTERSECTIONS
http://www.intersections.ro

4. CONCLUDING REMARKS

Eurocode [17] present four basic types of material behaviour to be used for FE analyses. However, no reference is made to cyclic loading and the document do not offer information regarding the cyclic behaviour of steel. The use of these material models with isotropic and/or kinematic hardening rules alone can give unsatisfactory results. Moreover, the use of uniaxial test raw results i.e. engineering or true stress-strain data might not be suitable for modelling of cyclically loaded structures.

Even if various formulations are available for modelling the cyclic behaviour of ductile steels, the behaviour of specific structures cannot always be modelled by using data provided by other researchers. It was shown that using material data that was used to calibrate other models, do not give satisfactory results in this particular case. It has to be stressed that the numerical model have to be calibrated and validated against experimental results before it can be used for numerical simulations, sensitivity and parametric studies, etc.

The author have shown that the uniaxial test data might be sufficient for calibrating a cyclic behaviour material model that implies a combined kinematic/isotropic hardening.

Acknowledgements

This work was partially supported by the strategic grant POSDRU/159/1.5/S/137070 (2014) of the Ministry of National Education, Romania, co-financed by the European Social Fund – Investing in People, within the Sectoral Operational Programme Human Resources Development 2007-2013.

References

1. Dahlberg M., Segle, P., Evaluation of models for cyclic plastic deformation – A literature study, *Report number: 2010:45*, 2010
2. Araujo, M., C., Non-Linear Kinematic Hardening Model for Multiaxial Cyclic Plasticity, *Thesis within Louisiana State University and Agricultural and Mechanical College*, 2002
3. Prager, W. *A New Method of Analyzing Stresses and Strains in Work Hardening Plastic Solids.* Journal of Applied Mechanics, Vol 23, pp. 493-496, 1956
4. Mroz, Z. On the Description of Anisotropic Work Hardening. *Journal of the Mechanics and Physics of Solids*, Vol 15, pp. 163-175, 1967
5. Besseling, J.F. A Theory of Elastic, Plastic and Creep Deformations of an Initially Isotropic Material. *Journal of Applied Mechanics*, Vol 25, pp. 529-536, 1958
6. Dafalias, Y.F. and Popov, E.P. Plastic Internal Variables Formalism of Cyclic Plasticity. *Journal of Applied Mechanics*, Vol 43, pp. 645-650, 1976
7. Armstrong, P.J. and Frederick, C.O. A Mathematical Representation of the Multiaxial Bauscinger Effect. *CEGB Report No. RD/B/N 731*, 1966

ISSN 1582-3024

8. Chaboche, J.L. Time-Independent Constitutive Theories For Cyclic Plasticity. *International Journal of Plasticity*, Vol 2, pp. 149-188, 1986
9. Chaboche, J.L. On Some Modifications of Kinematic Hardening to Improve the Description of Ratcheting Effects. *International Journal of Plasticity*, Vol 7, pp. 661-678, 1991
10. Ohno, N. and Wang, J.-D. Kinematic Hardening Rules with Critical State of Dynamic Recovery, Part I: Formulations and Basic Features for Ratcheting Behavior. *International Journal of Plasticity*, Vol 9, pp. 375-390, 1993
11. Bari, S., Constitutive Modeling for Cyclic Plasticity and Ratcheting, PhD thesis within the Department of Civil Engineering North Carolina State University, 2001
12. Hibbit. D., Karlson, B. and Sorenso, P (2007), ABAQUS User's Manual, Version 6.9
13. Lemaitre, J., and Chaboche J.-L., Mechanics of Solid Materials, *Cambridge University Press*, 1990.
14. Charles S., W., A Combined Isotropic-Kinematic Hardening Model for Large Deformation Metal Plasticity, U.S. Army Materials Technology Laboratory, Watertown, Massachusetts 02172-0001, 1988
15. Dinu F., Dubina, D., Neagu C., Vulcu C., Both, I., Herban S., Marcu D., Experimental and Numerical Evaluation of a RBS Coupling Beam For Moment Steel Frames in Seismic Areas, *Steel Construction Volume 6, Issue 1*, 27–33, 2013
16. European Convention for Constructional Steelwork, Technical Com-mittee 1, Structural Safety and Loadings; Working Group 1.3, Seismic Design. *Recommended Testing Procedure for Assessing the Behavior of Structural Steel Elements under Cyclic Loads*, First Edition, ECCS 1986
17. EN 1993-1-5: Eurocode 3: Design of steel structures - Part 1-5: General rules - Plated structural elements
18. Elkady, A., Lignos, G., D., Analytical investigation of the cyclic behavior and plastic hinge formation in deep wide-flange steel beam-columns, DOI 10.1007/s10518-014-9640-y, published online 2014
19. Terry P., Nonlinear response of steel beams, National Technical Information Service, *Operations Division, 5285 Port Royal Road, Springfield, Virginia 22161 - DSO-00-01*, 2000
20. Halama, R., Sedlák, J., & Šofer, M. Phenomenological Modelling of Cyclic Plasticity. Intech International, 1, 2012
21. Collin, J. M., Parenteau, T., Mauvoisin, G., & Pilvin, P. Material parameters identification using experimental continuous spherical indentation for cyclic hardening. Computational Materials Science, 46(2), 333-338, 2009

ISSN 1582-3024